Assessment on the CO_2 Geological Sequestration into Deep Coal-bearing Formation Using Numerical Fluid Dynamics Simulation

Supervisor: Asso. Prof. Shimada Sohei

Dept. Environment Systems 47-086661 Chai Zhenjie Graduation Date: March 2010

Key Words: Deep Saline Aquifer, Unminable Coal Seam, CO_2 Geological Storage, Simulation

1. Introduction

CO_2 geological storage (CGS) has been recognized as an indispensible and cost-efficient abatement measure against the Global Warming due to the CO_2 emission from large-scale energy-related sources. Within the CGS, disposal of CO_2 into deep saline aquifer formation (DSAF) and injection of CO_2 into deep unminable coal seam (UCS) for enhanced coalbed methane recovery (ECBMR) are two promising technologies which have been widely studies.

Recently, the interest of geologists and policy-makers in a specific type of subsurface formation called deep coal-bearing formation (DCBF) is booming. DCBF is characterized by the generation of relatively thin coal seam between strata of other subsurface materials, mostly sandstone. It deserves special attentions because of its intrinsic saline-aquifer-like characteristics resulting from the huge amount of storage potential all around the world as well as the presence of coal which may reduce the risk of the leakage and offset the operation cost by ECBMR.

However, currently while the geological surveys on DCBF are being widely conducted, no one has ever performed any numerical simulation on this type of formation for investigation on the impact on CO_2 storage in such integrated formation. Undoubtedly, there must be mutual enhancement effects or mutually adverse interaction between the coal seam and other strata on the overall performance of CO_2 storage corresponding to the different injection production profiles, time scale and geological conditions and so far, these issues remain concealed.

Base on the discussion above, the objective of this study is to develop a numerical simulator and apply it on the comprehensive study on CO_2 storage in DCBF to reveal the real behavior of CO_2 along with other side-substances (e.g. methane, nitrogen) inside a well-defined DCBF reservoir, and to assess the overall performance of CO_2 storage.

2. Numerical Simulator Development and Implementation

Considering the requirements for the description of CO_2 storage into DCBF, which actually combines all the basic frameworks in the individual case for DSAF and ECBMR he conceptual structure of the model is shown in Figure 3. with the multi-phase multi-component flow profiles on the left and the injection-projection profile on the right.

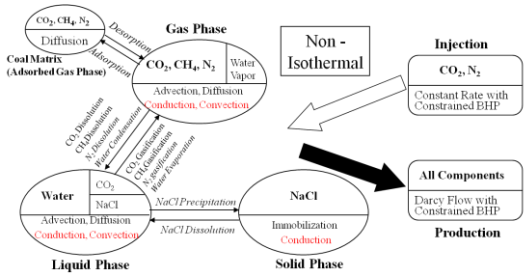

Figure 1. Structure of Multiphase Multicomponent Fluid Model

The whole system in this study, as depicted in Figure 1 comprises as many as three phases (i.e. Gas, Liquid, Solid) and five components (CO_2, CH_4, N_2, NaCl, Water) on the assumption of non-isothermal condition. In Figure 1, each ellipse represents one single phase respectively except for the upmost one which stands for the gases in adsorbed state in the coal's secondary porosity (coal matrix) and the interporosity diffusive flow (between matrix and cleats) is treated as the single-phase sink (adsorption) and/or source (desorption) term in the governing equations of CO_2, CH_4 and N_2 that will be presented later. Arrow lines along with the process denotations linking the pairs of phases

account for the phase transitions and phase changes that may occur dominantly in the scope of this study. As for each ellipse (3 phases and one adsorption state), all the components that may appear in that phase/state to the extent of a certain significant concentration are collected in the upper halves and the components in bold characters stand for the rich components in that phase/state. Then, the lower halves of the circles account for the main massive transport (black) and heat transfer (red) of that phase/state in the porous media of DCBF from the macroscopic point of view. On the right part of Figure 1, two rectangles provide an image of injection-production profiles. Similar to the way of expression in phases, the upper parts consist of the components involved and the lower parts explain the transport mechanisms near the wellbores. The fluid flows from/to the wellbores are regarded as source and/or sink terms in the governing equation like sorption process. Since the simulation is run in the infinitesimal time step, the fluid system is presupposed to keep in the state of thermodynamic equilibrium locally inside every grid (which depends on the space discretization strategy) for every time step.

1. Primary Variables

According to Gibbs' Law, for this study with non-isothmal condition, there should be as many as 6 primary variables and consequently 6 governing equations.

2. Governing Equation

In this study, for a multi-phase multi-component system with DOF of 6, six governing equations are required to set up a system of equations with six unknown primary variables. Five equations based on the mass balance equation are given to five components respectively and the rest one accounts for the energy conservation in the system. All the values of dependent variables in the governing equation are volumetric averages over the corresponding representative elementary volume (REV) [Garcia, 2003], which in this study is equivalent to the individual grid volume. The governing equation for CO_2 for examples

$$\frac{\partial}{\partial t}(\phi S_g b_g t_g^c + \frac{\phi S_l \rho_l w_l^c}{\rho_{STP}^c}) - \boldsymbol{F}_{l,adv}^c - \boldsymbol{F}_{l,dif}^c - \boldsymbol{F}_{g,adv}^c - \boldsymbol{F}_{g,dif}^c - \boldsymbol{q}_l^c - \boldsymbol{q}_g^c = 0$$

where

$$\boldsymbol{F}_{g,adv}^c = \nabla \cdot \left[\frac{b_g \vec{K} k_{rg} t_g^c}{\mu_g}(\nabla P_g - \rho_g \vec{g})\right] \quad \boldsymbol{F}_{l,adv}^c = \nabla \cdot \left[\frac{\rho_l \vec{K} k_{rl} w_l^c}{\mu_l \rho_{STP}^c}(\nabla P_l - \rho_l \vec{g})\right]$$

$$\boldsymbol{F}_{l,dif}^w = \nabla \cdot \left(\frac{\phi S_l \tau_l \rho_l D_l^c \nabla w_l^c}{\rho_{STP}^c}\right)$$

$$\boldsymbol{F}_{g,dif}^w = \nabla \cdot (\phi S_g \tau_g b_g D_g^c \nabla t_g^c)$$

$$\boldsymbol{q}_{matrix}^c = -\frac{1}{tau}(C^c - C_{matrix}^c)$$

3. Discretization

The method used in this study for discretization is finite-difference method.

For example, to dicretize the governing equation of CO_2 described above:

Assume:

$$M_g^c = \phi S_g b_g t_g^c \qquad M_l^c = \frac{\phi S_l \rho_l w_l^c}{\rho_{STP}^c}$$

Time discretization (backward scheme) yields:

$$\frac{\partial}{\partial t}(M_g^c + M_l^c)\Big|_{dis} = \frac{M_g^c\big|^{t_k+\Delta t} + M_l^c\big|^{t_k+\Delta t} - M_g^c\big|^{t_k} - M_l^c\big|^{t_k}}{\Delta t}$$

The space discretiztion in the vertical direction (central difference scheme) yields:

$$\nabla \cdot \left[\frac{b_g \vec{K} k_{rg} t_g^c}{\mu_g}(\nabla P_g - \rho_g \vec{g})\right]\Big|_{dis}$$
$$= \frac{1}{\Delta z}\left[(b_g k_{rg} t_g^c)\big|_{uw}^{in_+}\frac{K_z}{\mu_g}\Big|_h^{in_+}\frac{P_g\big|^{z+1} - P_g\big|^z + (\rho g z)\big|_a^{in_+}}{\delta z_+}\right.$$
$$\left. + (b_g k_{rg} t_g^c)\big|_{uw}^{in_-}\frac{K_z}{\mu_g}\Big|_h^{in_-}\frac{P_g\big|^{z-1} - P_g\big|^z + (\rho g z)\big|_a^{in_-}}{\delta z_-}\right]$$

where z-1,z,z+1 represents three vertically adjacent grids. The source/sink terms in every governing equation do not need discretizing, because they are scalar quantities without orientations. However, it is highly required that all of them are evaluated at the new time step, $t_{k+1} = t_k + \Delta t$. This ensures the numerical stability

needed for an efficient calculation of multiphase flow [Peaceman, 1977].

4. Covergence condition

Newton-Raphson iteration method is applied here to solve the discretized differential equation. Convergence condition is set as $\left|\frac{R_e^c}{M_g^c + M_l^c}\right| \le 10^{-7}$

3. Simulator Verification

The newly-developed simulator is verified by comparing the result to other results calculated by other advanced simulators regarding the following the guideline [3].

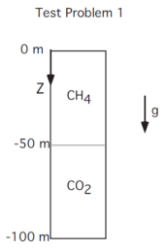

1. Test Problem 1

The test problem 1 creates a vertical one-dimensional reservoir to test the binary gas mixture for CO_2 and CH4 in it. The reservoir contains only residual water. It considers the mixing by molecular diffusion and advection of a stably stratified one-dimensional column 100 m in height with the light gas (CH_4) on the top and the heavy gas (CO_2) on the bottom (Figure). The test is used to mainly check the thermodynamic properties of CO_2 and CH_4 as well as the gas mixture.

The result is shown in Figure 2 by means of the CO_2 mole faction.

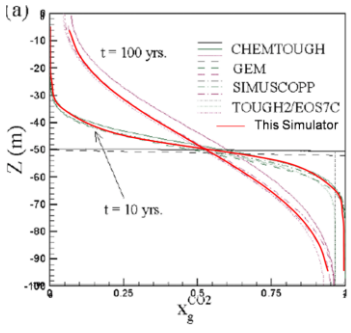

Figure 2 Comparison Result

The result shows an excellent agreement with the results from other simulators.

2. Test Problem 2

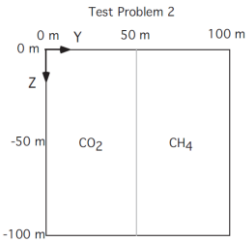

Figure 3 Schematic view of test problem 2

Properties		Initial Condtions	
Permeability	1. 0 x 10^{-14} m^2	Pressure at the top of domain	40 bars
Porosity	0.1	Temperature	40 °C
Touosity	1		
Molecular Diffusivity	1. x 10-7 m^2/s		
Residual Liquid Saturation	0.1		
Relative Permeability of Liquid	0	Boundary Conditions	
Relative Permeability of gas	Linear model	All boundaries are closed	

Table 1 Initial condition for test problem 2.

Test problem 2 is used to check the density-driven flow resulting from the density difference in these two substances. The schematic view the reservoir model and the initial condition of this test are given in Figure 3 and Table 2. The result is shown in a density filed graph form (Figure 4).

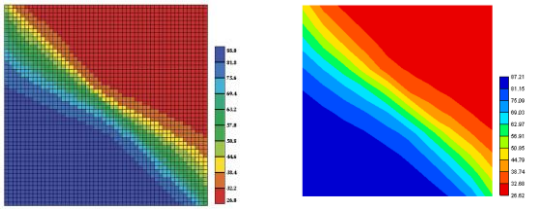

4. Application on DCBF and Studies

1. Evaluation Index

In order to compare the case by case quantitatively, several evaluation indexes are defined in advance for two different aspects, CH4 production and CO2 storage.

R_{CH4} = ratio of methane recovered;

S_{CH4} = (the amount of CH4 in gas phase)/(produced CH4);

A_{CO2} = (adsorbed CO2)/(CO2 injected)

F_{CO2} = (CO2 in gas phase)/(CO2 injected)

$$OP = \frac{Total\ amout\ of\ gases\ in\ gas\ phase}{CH4\ proudction\ amount + CO2\ injection\ amount}$$

2. Reservoir Model 1

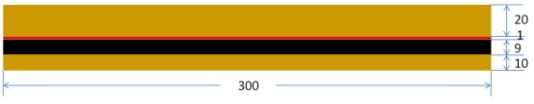

Figure 5 Schematic View of Reservoir Model 1

Reservoir model 1 consists of one layer of coal

seam coupled by a thin layer of shale lying directly over it. The top and bottom of the model are two sandstone formations.

Assuming that CO2 is injected into different strata, one is into the coal seam, the other one is injected into the sandstone layer below the coal seam. The resultant data representing the partition of CH4 and CO2 into different phases (gas phase, liquid phase, adsorbed state, production) storage at the end of the simulation (100 year)are shown in Figure 6,7 with the list of evaluation indexes given in Table 3.

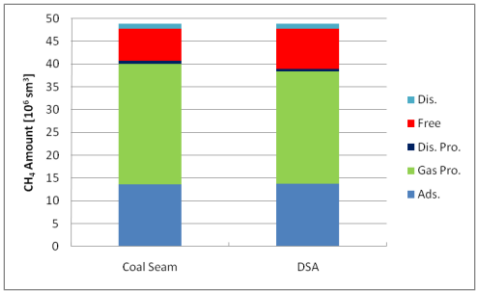

Figure 6 Partition of CH4 in different phases.

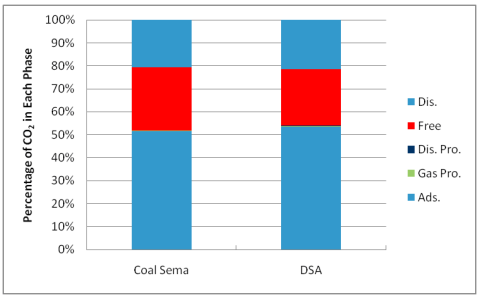

Figure 7 The percentage of CO2 in different phase

Table 2 Evaluation Indexes

CH_4	Coal Seam	DSA		CO_2	Coal Seam	DSA
R_{CH4}:	0.5552	0.5173		A_{CO2}:	0.5146	0.5353
S_{CH4}:	0.2664	0.3538		F_{CO2}:	0.2755	0.2443
OP:	0.2479	0.2301				

It suggested by the index figure that the injection in the sandstone will have a high overall performance.

3. Reservoir Model 2

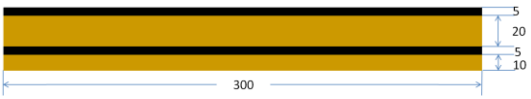

Figure 8 Schematic View of Reservoir Model 2

Reservoir Model2 comprises two coal seams as illustrated in Figure 8. The thickness of the coal reduced to 5 m. Three placed have been chosen to for the CO2 injection, i.e. coal seam, lower sandstone and upper sandstone.

The results along with the primary production data and the corresponding evaluation indexes are shown in Figure 9,10 and Table 4.

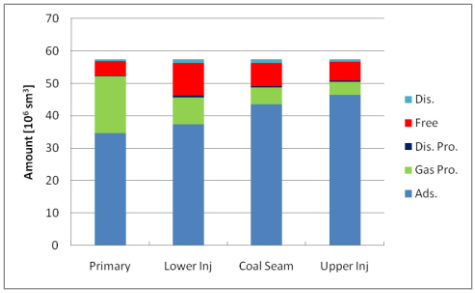

Figure 9 CH4 Partition in different phases

Table 3 CO2 Percentage in different phases

CH_4	Primary	Lower Inj	Coal Seam	Upper Inj		CO_2	Lower Inj	Coal Seam	Upper Inj
R_{CH4}:	0.3098	0.1526	0.0986	0.0799		A_{CO2}:	0.4128	0.3642	0.3063
S_{CH4}:	0.2527	1.2059	1.3508	1.3736		F_{CO2}:	0.3265	0.3781	0.4196
OP:	0.0770	0.2802	0.2870	0.3000					

The results show that ECBMR is not suitable for this type of DCBF.

4. Case Study

The model 2 is used to imitate the DCBF under the Ariake sea, Kyushu, Japan, since they have the similar structure. The geological and hydrological parameters are set to be same with that in Ariake as long as it is available. The results are shown in Figure 10.

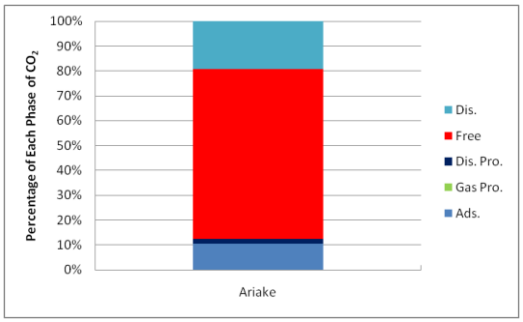

Figure 10 Percentage of CO2 in different phases

The large portion of CO2 remains in the gas phase after 200-year simulation. It can be explained by the low permeability of both the upper coal seam and the lower coal seam.